EXTENDED ABSTRACTS BOOK

EAGE 61st Conference and Technical Exhibition

Helsinki, Finland,

7 - 11 June 1999

POSTER PRESENTATIONS

Posters on display from 8 – 11 June

EAGE Business Office
Standerdmolen 10
PO Box 59
3990 DB Houten
The Netherlands

Telephone: + 31 30 6354066
Telefax : + 31 30 6343534

P027 INTERPRETATION OF RESISTIVITY SOUNDING DATA — DISTORTED BY GEOLOGICAL NOISE

VLADIMIR A. SHEVNIN, ALEXEY A. BOBACHEV,
IHOR N. MODIN and EUGENE V. PERVAGO
Moscow State University, Department of Geophysics, 119899 Moscow, Russia

The traditional resistivity sounding method deals with isolated sounding sites located casually on profile or area and executed with logarithmic step in distance growth. This technology has very restricted possibilities. Therefore it has begin to exchange practically simultaneously in different countries into new sounding technology, called multi-electrodic sounding, or resistivity tomography, electrical imaging, etc. Its main advantage - more dense survey along profile - is rather evident, while the other - overlapping system of measurements is not so visible. Our group in MSU began to apply multi-electrodic resistivity sounding, for the purpose not to increase field survey velocity or to transit to 2D interpretation, but to overcome distorting influence of geological noise. From the end of the 80-th we have been working in areas with high resistivity contrast along both vertical, and horizontal direction. Such sounding data have different features of distortions or differences from response for horizontally layered models. We developed software to establish VES data distortion with the help of various indicators, noticeable on VES curves. This is the brief list of such indicators or signs:

1. Signs for single non-segmented VES curve: a) when part of VES curve goes up at an angle more than 45°, b) when part of VES curve goes down more steep, than VES with μ=0; c) there are abrupt extremums or break points on VES curve, that are not coincide with theoretical one. 2. For segmented VES curve: great vertical gaps at segments' overlaps; crossing overlaps or any other their arrangement differs from theoretical one. 3. For VES profile: abrupt changes in form or level of VES curves, when distances between VES sites are smaller than maximum depth of investigation. 4. For the pair of pole-dipole VES curves, measured in the same point (AMN+MNB): differences in form of these curves.

The computer VES data analysis has shown, that more than 70 % of all VES curves are distorted. That means, that the distortions are practically constant features of resistivity sounding.

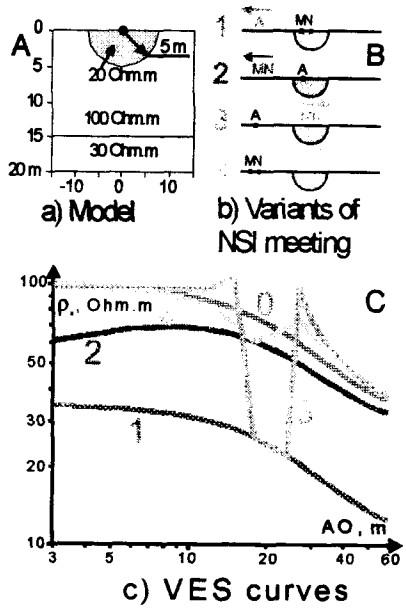

Fig.1. Model (A), variants of NSI meeting (B) and AMN sounding curves (C)

Carrying out the large volumes of VES field measurement and their interpretation (up to 1000 VES sites a year) we analyzed misfit errors of VES curves interpretation. The average value of misfit error (average RMS or $\sqrt{D}$, where D is dispersion) consists 8-12%, that seems rather high value and needs to be explained. The theory of geophysical interpretation (Tarhov et al., 1982) says that the total dispersion of geophysical field includes technological and geological dispersions, according to formula:

$$Dtotal = Dtechnol + Dgeol$$

Dtotal can be determined on background dispersion of geophysical field (in area without strong anomalies). Indirectly it is possible to estimate this value on misfit error. Dtechnol can be estimated on control measurements, and according to the instruction on resistivity method RMS measuring error should not exceed 5%. In practice measuring error depends on accuracy of measuring instrument (which does not exceed 2%) and on accuracy of electrodes' arrangement (geometrical error, which does not exceed 1-1.5%). Thus, the main factor of the differences between Dtotal and Dtechnol is geological noise Dgeol. Near-surface inhomogeneities (NSI) are the

main source of geological noise, because these are close to sites of current excitation and electrical field reception. The influence of near-surface inhomogeneities is analogous to "broken glass" or wavered see surface, prevented from clear seeing deeper objects through them. That is why we tried to investigate NSI influence, their typical anomalies and possibility of geological noise canceling from sounding data.

Fig.1 shows distortions caused by half-spherical NSI on electrical sounding curves for pole-dipole array AMN. The curve 0 corresponds to the case of two-layer model without NSI. The curves 1 - 4 correspond to various variants of AMN array elements' meeting with NSI (b). In case 1 unmovable dipole MN is placed at 3 m to the left of NSI center, and current electrode A moves to the left. In case 2 the single electrode A is at 3 m to the left from NSI center and dipole MN is moving away. In case 3 unmovable electrode A is placed out of NSI and dipole MN is going over NSI. In case 4 unmovable dipole MN is placed out of NSI and single electrode A is going over NSI.

Distortions in these four cases (c) are of two main types: 1) quasi conformable 2) unconformable. Quasi conformable distortions occur in cases 1 and 2, when unmovable element of array is in NSI limits. In these cases ρ_a curve only moves along ρ_a axis without changing its form. Unconformable distortions occur in cases 3 and 4, when moveable element of array is going over NSI. In these cases the form of some part of VES curve has changed at the moment of crossing NSI limits. Dipole element of array gives more strong distortion effects, than the single one.

We used to apply two-sided pole-dipole sounding array AMN+MNB with a reference point in the center of unmovable MN. For that case we use terms P- and C-effects to describe distortions.

P-effect is distortion from NSI placed near potential electrodes. Its analog is S-effect, known in MTS. P-effect shows itself as a "quasi-conformable" vertical shift of VES curve along ρ_a axis without its form changes. If VES curve is non-segmented, that P-effect can be found in comparison of this curve with the neighbors. For segmented curve P-effect gives the different shifts of segments for different MN with the total form of curve being conserved.

C-effect is distortion from NSI placed near current electrode. C-effect was found first in modeling results and only after that in field data. The main cause of that is in a difficulty of finding C-effect on a single curve and on ρ_a pseudo-cross-section when all VES were measured with a logarithmic distance step. Fig.2 shows results of modeling VES along profile over two-layered structure with one NSI (from fig.1) (2,a - ρ_a pseudo cross-section and 2,b - so-called V-transformation or a vertical derivative of ρ_a curves (along AO axis). On fig.2,a there is clear visible P-effect (as vertical zone) and weakly visible C-effect (seeing by distortions of isolines to the right and down from the vertical zone). V-transformation (fig.2,b) make P- effect invisible (as conformable distortion) and C-effect clear visible (due to its unconformability).

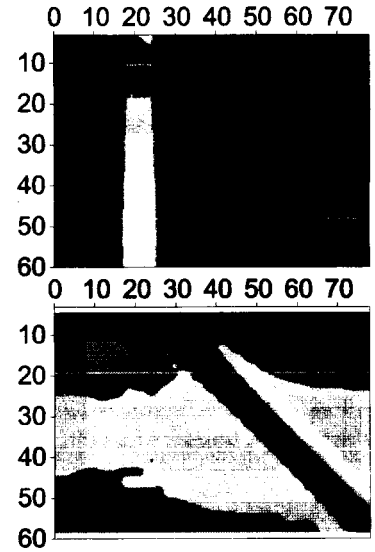

Fig.2. ρ_a field and its V-transformation for one half-spherical NSI model from fig.1.

C-effect has several particularities, which do it more dangerous, than P-effect: a) It changes form of VES curve. b) On ρ_a cross-section C-effect shows itself as dipping layer. To make it regular and clear visible we apply multi-electrodic sounding with linear step in distance growth exactly equal to sounding step along profile, linear scale along AO axis to display pseudo cross-sections and V-transformation for C-effect visualization.

When standard VES technology is used NSI's distortions are weakly visible, and their danger is underestimated. We collected a set of case histories, when typical NSI distortions were interpreted as geological objects. The greatest NSI influence is in urban areas, in places with an artificial upper layer, near trenches with cables and tubes. Canceling of their distorting influence will help to arise geological effectivity of VES method.

Fig.3 shows the occurrence of C-effect, resulted from one NSI for measurements with different MN positions and one electrode A moving over NSI. Point of reference is in MN location. By choice of linear scale along AO distance axis on ρ_a cross-section C-effect produces a linear zone of distortion, inclined under 45°. As the AO distances interval begins with some R_{MIN}, and ρ_a cross-section is drawn from that level (fig.3), C-effect anomaly comes to this level not in a point of the actual NSI situation, but on a

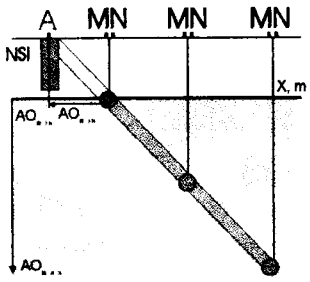

Fig.3. The scheme of C-effect origin.

distance R_{MIN} from it, that is taken into account on fig.4. Fig.4 displays distorting effects, caused by NSI on ρ_a cross-sections for different arrays. Cases 2 and 4 correspond to pole-dipole arrays AMN and MNB, with reference point in the center MN. The hit of MN in NSI location produces P-effect, and the hit of the current electrodes A or B produces C-effects. For

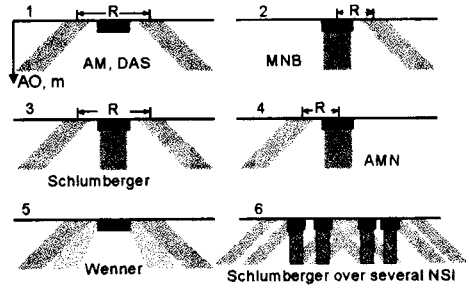

Fig.4. Effects of distortions (vertical and inclined lines) from NSI (black rectangulars) for different arrays.

Schlumberger array (case 3) on ρ_a cross-section from each NSI three lines of distortions arises (the vertical zone of P-effect and two zones of C-effect, going away from NSI with AO growth. For several NSIs (case 6) distorting effects crosses each other, and as a result, a level of geological noise is increasing and the possibility of VES data correlation worsened down to loss an opportunity to trace real boundaries on VES data. The case 1 on fig.4 corresponds to AM and ABMN arrays with the reference point in the center of array. The current and receiving elements of arrays are here equivalent, therefore NSI causes occurrence of two lines of distortions, inclined under 45°. Distortions for Wenner array, used in Electrical Imaging technology are the most difficult in a pattern (case 5 on fig.4). As moving rate for MN electrodes is less, than for AB, the distortions for MN electrodes on ρ_a cross-sections incline at angles more than 45°.

As P-effect is conformable, it does not give the essential contribution in misfit error at interpretation, though it influences on boundaries' correlation along profile. Main contribution in misfit error gives C-effect. It has weaker amplitude, than P-effect. If we remove both effects, the improvement will be even more significant, than it is possible to see on change of misfit error.

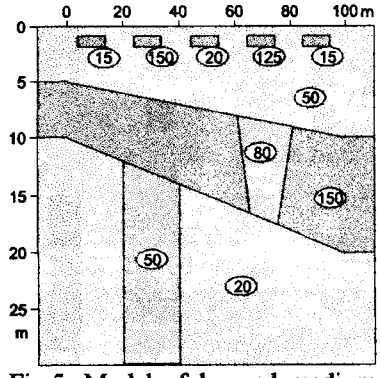

Fig.5. Model of layered medium with deep objects and NSI.

Fig.5 shows the central part of complex model with layering, deep objects and NSI. ρ_a fields for AMN and MNB arrays (fig.10,C) are strongly distorted by influence of NSI, deep objects and inclined boundaries.

If ρ_a data from fig.10,C we transform to AMNB array and carry out 1D interpretation, the form of boundaries will appear strongly distorted (boundaries look as if these are studied through the broken glass) (fig.6, a). After canceling distortions with Median algorithm (see below), 1D interpretation will give boundaries with much greater accuracy (fig.6, b). To estimate data processing quality we can compare misfit errors of VES curves interpretation before and after canceling distortions (fig.7). Both on modeling and experimental data we established, that after canceling distortions the error of interpretation becomes appreciably reduced.

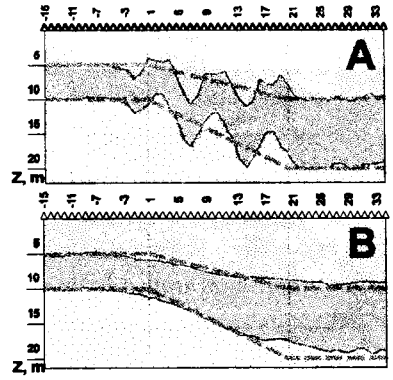

Fig.6. Comparison of VES 1D interpretation's results for model from fig.4 before and after distortions filtering.

The misfit error for practical data interpretation decreases in 4-5 times from 8-12% up to 2-3%. It gives great improvement of VES quality and narrowing of equivalence principle limits. After removal of distortions caused by NSI the interpretation accuracy comes nearer to accuracy of the used instrument. That in turn give us possibility to apply more precise measuring instrument.

Algorithm Median and principles of its operation.

Algorithm Median has been developed by E.Pervago in 1994. The program name is a result of application median

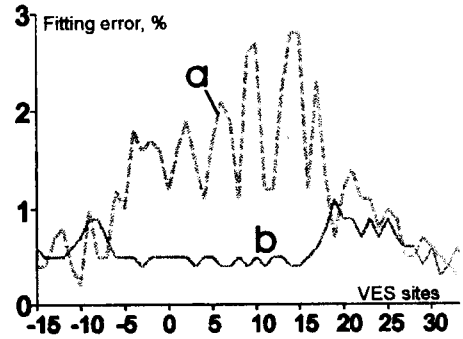

Fig. 7. RMS misfit errors of VES interpretation before (a) and after (b) filtering

polishing algorithm by J.Tukey at some stages of data processing. Block-scheme of Median program presented on fig.8. The algorithm works in three stages. At the first stage ρ_a fields for AMN and MNB arrays are divided into components: horizontally layered (HL), C, P and residuals R. As in the case of old building restoration made by archaeologists, the process includes decomposition into blocks, clearing each block, and then reconstruction from the cleared blocks. The process of decomposition on blocks is the most problematic part of algorithm. Decomposition is linear process, while the whole 2D resistivity problem is non-linear. The distortions from NSI are displayed as a regular noise, which can be canceled by the directional filtering. The distortions' pattern depends not only on local inhomogeneity, but also from a background structure. It is necessary to cancel distortion and not to deform a background part of the field. For that Median algorithm was tested and polished on many different models.

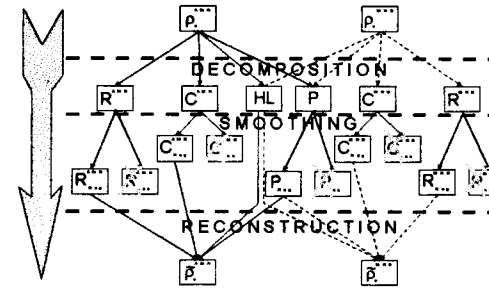

Fig.8. The scheme of algorithm Median.

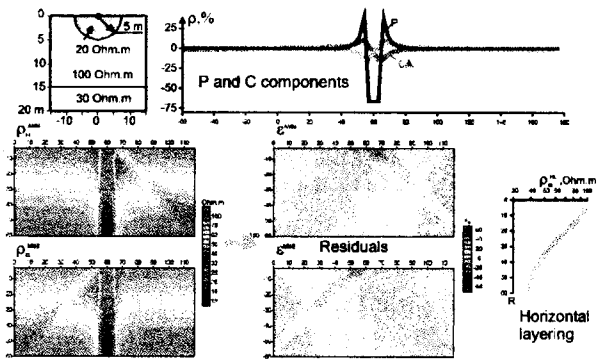

Fig.9. An example of ρ_a field decomposition for the model from fig.1.

Fig.9 shows decomposition of ρ_a field near hemispherical NSI above layered model. In this case P and C effects are local and their removal is very simple operation. Non-linear part of the field at reconstruction is conserved with the help of residuals. Layered component has clear physical meaning

Fig.10 shows more complicated example of ρ_a field decomposition. In this case P and C effects include both local and regional components (fig.10, D). Median polishing cancels local components while regional ones are used in reconstruction process.

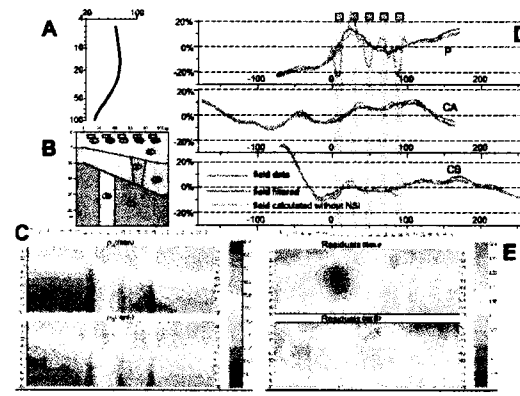

Fig.10. An example of ρ_a field decomposition for the model from fig.5.

The multi-electrodic soundings stimulated transition to 2D interpretation (Loke and Barker, Stoyer). Our researches of distortion's principles and the algorithm of noise removal, gives the greater application of 1D interpretation. In many cases ρ_a field seemed 2D only due to distortions. We want to say that the role of geological noise is huge. But its influence can be made regular with the help of correct field measuring technology. This situation is similar to that in reflection seismics. Theoretically it is possible to receive reflection with a single geophone and then to interpret it and to estimate depth of reflector. Large groups of geophones and enhanced measuring and data processing technologies in reflection seismics are used mainly for canceling false waves and different sources of geological noise. Interpretation begins only after data processing and canceling distortions. Now there is similar possibility in resistivity sounding. After filtering process models of interpretation become simpler. Many details near the earth surface now become removed and do not use for interpretation. Only effects of deep objects remain, and these are objects of our interest. The process of calculation becomes accelerated. We need to estimate smaller amount of parameters. Canceling geological noise give us a great chance to raise VES data quality and accuracy of their interpretation.

The references.

Tarhov A.G., Bondarenko V.M., Nikitin A.A. Integrated geophysics. M., Nedra. 1982. 293 pp.
Electrical prospecting by resistivity method. MSU edition, Moscow, 1994, 160 pp. (In Russian).
Loke M.H. and Barker R.D. Least-squares deconvolution of apparent resistivity pseudosections. Geophysics. Vol.60, No 6, 1995, p.1682-1690.